Collectivity in small and large collision systems at the LHC with ALICE

Katarína Křížková Gajdošová (for the ALICE Collaboration)
Faculty of Nuclear Sciences and Physical Engineering, Czech Technical University in Prague, Břehová 7, 115 19 Prague, Czech Republic

Abstract. Interactions of protons (pp) or of a proton with a lead nucleus (p–Pb) were not expected to form a deconfined hot and dense matter, called the Quark-Gluon Plasma (QGP), which is instead produced in heavy-ion collisions. However, high-multiplicity events in small collision systems exhibit signs of collectivity, which are understood as a signature of the QGP emergence in heavy-ion collisions. An excellent tool to probe the presence of collectivity is the anisotropic flow measured with two- and multi-particle cumulants. In these proceedings, we present the first measurement of flow coefficients and their magnitude correlations using symmetric cumulants for charged particles in pp collisions at centre-of-mass energies of $\sqrt{s} = 13$ TeV, p–Pb at $\sqrt{s_{\rm NN}} = 5.02$ TeV, Xe–Xe at $\sqrt{s_{\rm NN}} = 5.44$ TeV and Pb–Pb collisions at $\sqrt{s_{\rm NN}} = 5.02$ TeV, collected during the LHC Run 2 programme. In addition, the flow coefficients of identified particles in p–Pb collisions are shown. Such a broad spectrum of colliding systems with different energies and a wide range of multiplicity allows for a detailed investigation of their collision dynamics. Non-flow effects, which are azimuthal correlations not originating from a common symmetry plane, are suppressed with the pseudorapidity separation and the subtraction method. These results provide an important insight into the nature of collective phenomena in different collision systems.

1. Introduction

Heavy-ion collisions at ultrarelativistic energies are used to create a state of strongly-interacting matter called the Quark–Gluon Plasma (QGP), where quarks and gluons are in a deconfined state. In a hydrodynamic picture, the collective evolution of this medium translates the initial spatial anisotropies in the overlap region of the colliding heavy nuclei into an anisotropy of final-state particles. To characterise the anisotropy, the azimuthal distribution of emitted particles can be decomposed into a Fourier expansion relative to a common symmetry plane Ψ_n with anisotropic flow coefficients $v_n = \langle \cos [n(\varphi - \Psi_n)] \rangle$ [1]:

$$\frac{dN}{d\varphi} \propto 1 + 2 \sum_{n=1}^{\infty} v_n \cos [n(\varphi - \Psi_n)]. \tag{1}$$

The flow harmonics v_n thus quantify the preferred direction of emitted particles, and represent a collective response of the QGP to the initial spatial anisotropies, which makes them one of the most suitable probes to study the properties of this medium. An extensive set of measurements of anisotropic flow performed at the Large Hadron Collider (LHC), together with quantitative model comparisons have improved our knowledge about the QGP [2, 3, 4, 5, 6, 7, 8]. It is now well established that this medium behaves like a nearly perfect, collectively expanding liquid;

this behaviour manifests itself in the form of long-range multi-particle correlations between the final-state particles.

Small collision systems, such as pp or p–Pb collisions, were originally considered to lack the conditions necessary to create a hot and dense medium such as the QGP. However, recent measurements of anisotropic flow revealed features, similar to those observed in heavy-ion collisions, that are believed to indicate the presence of the QGP. In particular, measurements of two-particle correlations as a function of the pseudorapidity difference $\Delta\eta$ and the azimuthal angle difference $\Delta\varphi$ revealed a near side "ridge" structure in high-multiplicity pp and p–Pb collisions [9]. A negative sign of the four-particle cumulant was also observed at high multiplicity in collisions of small systems [10]. Measurements of p_{T}-differential flow coefficients for identified particles in high multiplicity p–Pb collisions showed a hint of a mass ordering at low p_{T}, and a baryon-meson grouping at intermediate p_{T}, which is understood as a consequence of hydrodynamic flow and partonic collectivity in heavy-ion collisions [11]. Whether these similarities with heavy-ion collisions, also observed in small collision systems, originate from the same mechanisms is yet to be understood. Phenomenological models with a hydrodynamic description of the system evolution are able to describe measurements obtained with two-particle correlations [12, 13, 14, 15, 16]. However, other alternative scenarios, including correlations of gluon fields in the initial stages of a collision, are also able to qualitatively reproduce some features of the results of flow coefficients [17, 18, 19]. Therefore, new measurements that are able to disentangle between various theoretical approaches, are of great necessity.

The study presented here shows the ALICE measurements of flow coefficients and their correlations as a function of multiplicity in a variety of collision systems [20], and new p_{T}-differential measurements of numerous identified particle species in p–Pb collisions [21]. All the results are extracted using the latest techniques to suppress non-flow contamination as much as possible, which makes the comparison to future theoretical calculations straightforward.

2. Analysis method

The analysed data samples were recorded by ALICE [22] during the LHC Run 2 period. In particular, data from Pb–Pb collisions at centre-of-mass energies $\sqrt{s_{\mathrm{NN}}} = 5.02$ TeV, Xe–Xe collisions at $\sqrt{s_{\mathrm{NN}}} = 5.44$ TeV, p–Pb collisions at $\sqrt{s_{\mathrm{NN}}} = 5.02$ TeV and pp collisions at $\sqrt{s} = 13$ TeV were selected. Minimum-bias triggered events, based on a coincidence of signals between the two arrays of the V0 detector (V0A and V0C), were used in all collision systems except for pp collisions. In this collision system, a dedicated trigger, selecting approximately 0.1% of the largest multiplicity events based on the amplitude in both arrays of the V0 detector, was applied. Events that passed the trigger threshold had 4 times larger multiplicity in the V0 acceptance than the minimum-bias average. The selected data samples were further reduced from pileup and background events. Overall, the results from the analyses with charged particles were obtained from 3.1×10^8 high-multiplicity pp, 2.3×10^8 p–Pb, 1.3×10^6 Xe–Xe and 5.5×10^7 Pb–Pb collisions, while 6.0×10^8 minimum bias p–Pb and 1.7×10^8 minimum bias pp collisions were used for the analyses with identified particles. These data samples were further divided into several event classes based on the multiplicity distribution measured with the V0A detector.

Charged tracks with a transverse momentum of $0.2 < p_{\mathrm{T}} < 3.0$ GeV/c and pseudorapidity $|\eta| < 0.8$ were used for the analyses. Particle identification of $\pi^{\pm}$, $\mathrm{K}^{\pm}$ and p($\overline{\mathrm{p}}$) was performed using a Bayesian approach [23] based on the signals from the Time Projection Chamber (TPC) and Time-of-Flight (TOF) detectors. Particles with a short life-time, $\mathrm{K}^0_{\mathrm{S}}$, $\Lambda(\overline{\Lambda})$ and ϕ, cannot be detected directly, but instead are reconstructed via their decay products on a statistical basis using the following decays: $\mathrm{K}^0_{\mathrm{S}} \to \pi^+ + \pi^-$, $\phi \to \mathrm{K}^+ + \mathrm{K}^-$ and $\Lambda \to \pi^- + \mathrm{p}$ ($\overline{\Lambda} \to \pi^+ + \overline{\mathrm{p}}$).

Measurements of multi-particle cumulants [24, 25, 26, 27] and symmetric cumulants [28] were calculated using the generic framework [28] with weighted Q_n-vectors, to correct for non-uniform acceptance and tracking inefficiencies.

Small collision systems are largely dominated by short-range few-particle correlations not related to the common symmetry plane, such as jets or resonance decays, generally denoted as "non-flow". Correlations between particles originating from non-flow effects contaminate our measurements, and may obscure the possible signal of global collectivity involving many particles. The sub-event method [29, 30] was employed in the measurements in order to suppress this bias. In this method, particle m-tuplets are taken from different sub-events separated by a pseudorapidity gap, which ensures a long-range separation betwen particles that are correlated.

In addition, a subtraction method at the cumulant level, using data from minimum bias pp collisions, was used in p_{T}-differential measurements to remove the remaining non-flow contamination, following the equation:

$$v_2^{\mathrm{pPb,sub}}(p_{\mathrm{T}}) = \frac{d_2^{\mathrm{pPb}}(p_{\mathrm{T}}) - k \cdot d_2^{\mathrm{pp}}(p_{\mathrm{T}})}{\sqrt{c_2^{\mathrm{pPb}} - k \cdot c_2^{\mathrm{pp}}}}. \tag{2}$$

Here, c_2 and d_2 represent the reference and the differential two-particle cumulants, respectively, and $k = \langle M \rangle^{\mathrm{pp}} / \langle M \rangle^{\mathrm{pPb}}$ is a scaling ratio of mean event multiplicities used for the estimation of non-flow effects to account for the different system sizes of pp and p–Pb collisions.

3. Results

Measurements of flow coefficients v_n of inclusive charged particles from pp, p–Pb, Xe–Xe and Pb–Pb collisions using the two particle cumulant method with a large pseudorapidity gap ($|\Delta\eta|$) to suppress non-flow effects are shown in Figure 1. Large collision systems (Pb–Pb and Xe–Xe) exhibit a strong multiplicity (N_{ch}) dependence of v_2, which is understood as a hydrodynamic response to the initial geometry of the overlapping region of the colliding nuclei at large and intermediate multiplicities. The strength of the interactions that are responsible for the transfer of the initial spatial anisotropies to the final state momentum anisotropies is reflected at low multiplicities. In addition, an ordering of flow coefficients $v_2 > v_3 > v_4$ is observed in the whole multiplicity range in both Xe–Xe and Pb–Pb collisions, except for the fluctuation-dominated region of very central collisions (with the highest multiplicity), where $v_2 \sim v_3$. In peripheral heavy-ion collisions (low multiplicities), the values of v_n become compatible with those measured in pp and p–Pb collisions. A weak N_{ch}-dependence of v_n is observed in both small and large collision systems in this region, except for v_2, which rises with multiplicity for $N_{\mathrm{ch}} \geq 50$ in Pb–Pb collisions, while the weak N_{ch}-dependence remains in pp and p–Pb collisions at similar multiplicity. An ordering of v_n is reported in small collision systems, similar to that observed in in Xe–Xe and Pb–Pb collisions.

Differential measurements of v_2 of inclusive charged hadrons $\mathrm{h}^{\pm}$ and several different species of identified particles in p–Pb collisions are reported in Figure. 2. The results are obtained with unprecedented precision as a function of p_{T} with a $|\Delta\eta| > 0.4$ separation and an additional non-flow subtraction. Similar to heavy-ion collisions, a clear mass ordering is observed for $p_{\mathrm{T}} < 2.5$ GeV/c. It suggests a strong radial expansion of particles with similar velocity, causing a push of the heavier ones to higher momenta. In the region of intermediate momenta $2.5 < p_{\mathrm{T}} \leq 6$ GeV/c, the v_2 of different particle species are grouped into two distinctive trends. Such a behaviour was also observed in heavy-ion collisions where it is understood as a consequence of parton coalescence [31] or recombination mechanism at the point of particle production [32]. Both observations and the trend, qualitatively consistent with hydrodynamic calculations [15, 16], suggest the presence of hydrodynamic collectivity in high-multiplicity p–Pb collisions.

Figure 3 presents measurements of $v_2\{m\}$ using higher order cumulants ($m > 2$) compared between small (pp and p–Pb) and large (Xe–Xe and Pb–Pb) collision systems. The existence of long-range multi-particle correlations in large collision systems is inferred from the consistency of the results from standard and subevent method ($v_2\{m\} \approx v_2\{m\}_{\mathrm{sub}}$) and of the results

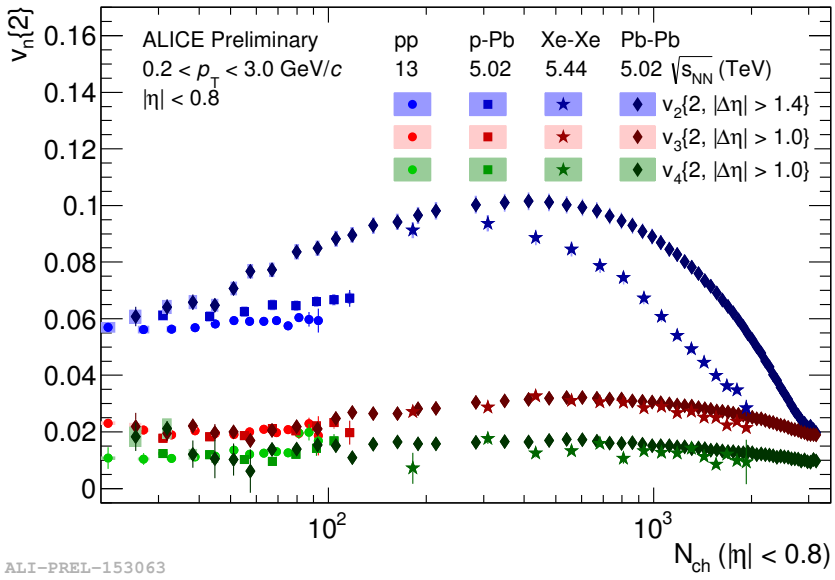

Figure 1. Multiplicity dependence of v_2, v_3 and v_4 measured using the two-particle cumulant method with a $|\Delta\eta|$ gap in small (pp and p–Pb) and large (Xe–Xe and Pb–Pb) collision systems.

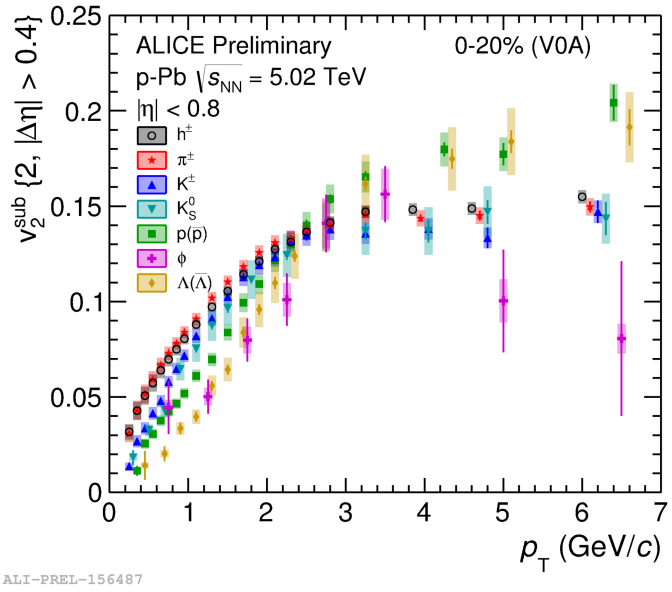

Figure 2. Transverse momentum dependence of $v_2^{\rm sub}\{2, |\Delta\eta| > 0.4\}(p_{\rm T})$ of $\rm h^{\pm}$, $\pi^{\pm}$, $\rm K^{\pm}$, $\rm K^0_S$, $\rm p(\overline{p})$, $\Lambda(\overline{\Lambda})$ and ϕ in p–Pb collisions in the $0-20\%$ V0A multiplicity class.

from cumulants of different orders ($v_2\{4\} \approx v_2\{6\} \approx v_2\{8\}$). In p–Pb collisions, the non-flow contribution to multi-particle cumulants can be further suppressed with the 3-subevent method, resulting in a decrease of the four-particle cumulant $c_2\{4\} > c_2\{4\}_{3-\rm sub}$. In turn, this leads to an increase of the flow signal $v_2\{4\}_{3-\rm sub} > v_2\{4\}$, based on the relation $v_2\{4\} = \sqrt[4]{-c_2\{4\}}$ [27]. A real-valued $v_2\{4\}$ could not be obtained in the largely non-flow dominated pp collisions. However, the contamination was successfully reduced with the 3-subevent method, leading to the first observed signal of $v_2\{4\}_{3-\rm sub}$ in pp collisions with ALICE and suggesting the

presence of multi-particle correlations even in pp collisions. The collective behaviour of small systems is further supported by compatible values of different orders of multi-particle cumulants $v_2\{4\}_{3-\mathrm{sub}} \approx v_2\{6\}$, observed in both pp and p–Pb collisions.

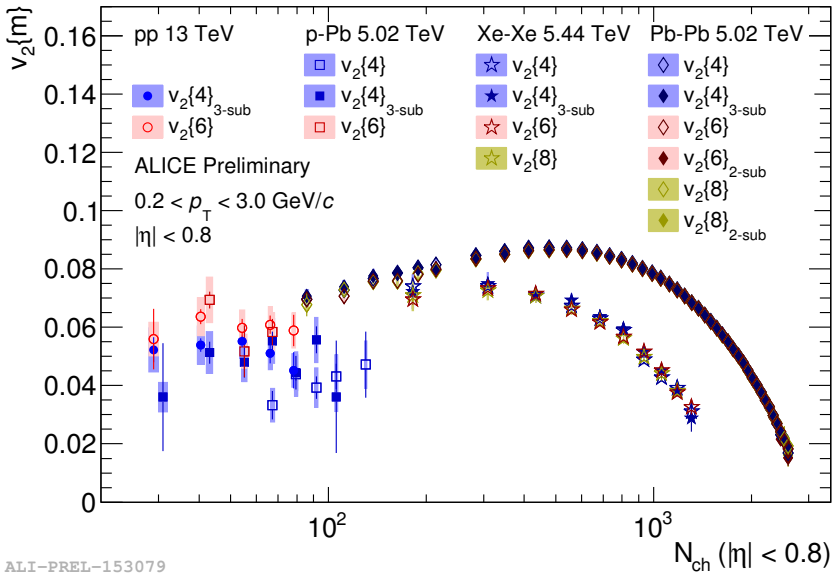

Figure 3. Multiplicity dependence of $v_2\{m\}$ for $m > 2$ in pp, p–Pb, Xe–Xe and Pb–Pb collisions.

The implications of the existence of long-range multi-particle correlations in small collision systems should be investigated with model comparisons. As it was mentioned in the Introduction, it is not yet clear which model scenario is the most suitable to describe the origin of these correlations in pp or p–Pb collisions. For that purpose, observables with a power to discriminate different model approaches are necessary. Symmetric cumulants (SC), in particular $\mathrm{SC}(3,2)$ and $\mathrm{SC}(4,2)$, provide access to the initial conditions and the dynamical evolution of the system [8]. Measurements of $\mathrm{SC}(m,n)$ with the 3-subevent method in pp, p–Pb, Xe–Xe and Pb–Pb collisions are reported in Figure 4. A positive $\mathrm{SC}(4,2)_{3-\mathrm{sub}}$ can be seen in the top panel, which is observed for all collision systems and in the entire multiplicity range. On the other hand, the $\mathrm{SC}(3,2)_{3-\mathrm{sub}}$ is negative at large and intermediate multiplicities for large collision systems, while there is a hint of a change to positive signs at $N_{\mathrm{ch}} \leq 90$. This trend seems to be followed by the results obtained in small collision systems.

4. Summary

We have presented new measurements of $v_2(p_{\mathrm{T}})$ using two-particle cumulants of inclusive and identified particles in high-multiplicity p–Pb collisions at $\sqrt{s_{\mathrm{NN}}} = 5.02$ TeV. In addition, the multiplicity dependence of v_n coefficients and their correlations in various collision system has been reported. The examined features of the measured results of flow coefficients in small collision systems and their striking similarity with measurements from large collision systems support the existence of collective phenomena in high-multiplicity pp and p–Pb collisions. The nature of these collective phenomena was further addressed by measurements of symmetric cumulants. The latter suggest that common mechanisms are responsible for the observations in small and large systems at similar multiplicities. All the results shown here provide an invaluable tool to further constrain the modelling of small collision systems and might allow us to understand the origin of collective effects in pp and p–Pb collisions.

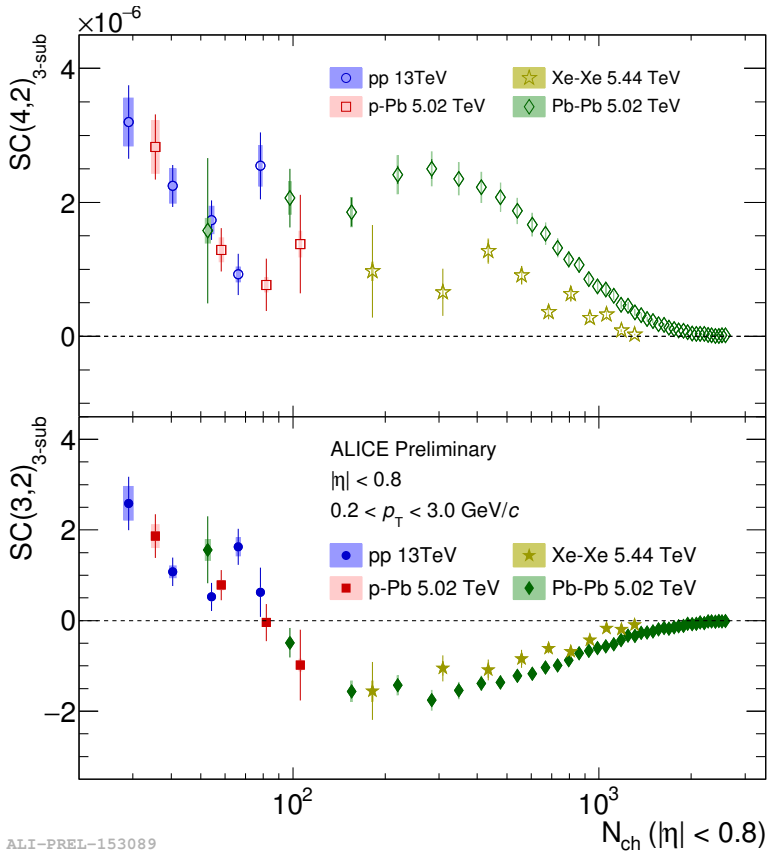

Figure 4. Multiplicity dependence of $SC(m,n)_{3-\mathrm{sub}}$ in pp, p–Pb, Xe–Xe and Pb–Pb collisions.

Acknowledgments

This proceeding are supported by the project Centre of Advanced Applied Sciences with the number: CZ.02.1.01/0.0/0.0/16-019/0000778. Project Centre of Advanced Applied Sciences is co-financed by European Union.

5. References

[1] Voloshin S and Zhang Y 1996 *Z. Phys.* **C70** 665–672 (*Preprint* hep-ph/9407282)
[2] Adam J *et al.* (ALICE) 2016 *Phys. Rev. Lett.* **116** 132302 (*Preprint* 1602.01119)
[3] Sirunyan A M *et al.* (CMS) 2019 *Phys. Lett.* **B789** 643–665 (*Preprint* 1711.05594)
[4] Acharya S *et al.* (ALICE) 2018 *JHEP* **07** 103 (*Preprint* 1804.02944)
[5] Acharya S *et al.* (ALICE) 2018 *Phys. Lett.* **B784** 82–95 (*Preprint* 1805.01832)
[6] Aaboud M *et al.* (ATLAS) 2018 *Eur. Phys. J.* **C78** 997 (*Preprint* 1808.03951)
[7] Acharya S *et al.* (ALICE) 2018 *JHEP* **09** 006 (*Preprint* 1805.04390)
[8] Adam J *et al.* (ALICE) 2016 *Phys. Rev. Lett.* **117** 182301 (*Preprint* 1604.07663)
[9] Khachatryan V *et al.* (CMS) 2010 *JHEP* **09** 091 (*Preprint* 1009.4122)
[10] Khachatryan V *et al.* (CMS) 2015 *Phys. Rev. Lett.* **115** 012301 (*Preprint* 1502.05382)
[11] Abelev B B *et al.* (ALICE) 2013 *Phys. Lett.* **B726** 164–177 (*Preprint* 1307.3237)
[12] Weller R D and Romatschke P 2017 *Phys. Lett.* **B774** 351–356 (*Preprint* 1701.07145)
[13] Mäntysaari H, Schenke B, Shen C and Tribedy P 2017 *Phys. Lett.* **B772** 681–686 (*Preprint* 1705.03177)
[14] Zhao W, Zhou Y, Xu H, Deng W and Song H 2018 *Phys. Lett.* **B780** 495–500 (*Preprint* 1801.00271)
[15] Werner K, Bleicher M, Guiot B, Karpenko I and Pierog T 2014 *Phys. Rev. Lett.* **112** 232301 (*Preprint* 1307.4379)
[16] Bozek P, Broniowski W and Torrieri G 2013 *Phys. Rev. Lett.* **111** 172303 (*Preprint* 1307.5060)
[17] Welsh K, Singer J and Heinz U W 2016 *Phys. Rev.* **C94** 024919 (*Preprint* 1605.09418)

[18] Dusling K, Mace M and Venugopalan R 2018 *Phys. Rev. Lett.* **120** 042002 (*Preprint* 1705.00745)
[19] Blok B and Wiedemann U A 2018 (*Preprint* 1812.04113)
[20] Gajdošová K (ALICE) 2019 *Nucl. Phys.* **A982** 487–490 (*Preprint* 1807.02998)
[21] Pacík V (ALICE) 2019 *Nucl. Phys.* **A982** 451–454 (*Preprint* 1807.04538)
[22] Aamodt K *et al.* (ALICE) 2008 *JINST* **3** S08002
[23] Adam J *et al.* (ALICE) 2016 *Eur. Phys. J. Plus* **131** 168 (*Preprint* 1602.01392)
[24] Borghini N, Dinh P M and Ollitrault J Y 2001 *Phys. Rev.* **C63** 054906 (*Preprint* nucl-th/0007063)
[25] Borghini N, Dinh P M and Ollitrault J Y 2001 *Phys. Rev.* **C64** 054901 (*Preprint* nucl-th/0105040)
[26] Borghini N, Dinh P M and Ollitrault J Y 2001 *International Workshop on the Physics of the Quark Gluon Plasma Palaiseau, France, September 4-7, 2001* (*Preprint* nucl-ex/0110016)
[27] Bilandzic A, Snellings R and Voloshin S 2011 *Phys. Rev.* **C83** 044913 (*Preprint* 1010.0233)
[28] Bilandzic A, Christensen C H, Gulbrandsen K, Hansen A and Zhou Y 2014 *Phys. Rev.* **C89** 064904 (*Preprint* 1312.3572)
[29] Jia J, Zhou M and Trzupek A 2017 *Phys. Rev.* **C96** 034906 (*Preprint* 1701.03830)
[30] Huo P, Gajdošová K, Jia J and Zhou Y 2018 *Phys. Lett.* **B777** 201–206 (*Preprint* 1710.07567)
[31] Molnar D and Voloshin S A 2003 *Phys. Rev. Lett.* **91** 092301 (*Preprint* nucl-th/0302014)
[32] Hwa R C and Yang C B 2003 *Phys. Rev.* **C67** 034902 (*Preprint* nucl-th/0211010)